Article

Dynamics of Xenon Binding Inside the Hydrophobic Cavity of Pseudo-Wild-type Bacteriophage T4 Lysozyme Explored through Xenon-Based NMR Spectroscopy

Herv Desvaux, Lionel Dubois, Gaspard Huber, Michael L. Quillin, Patrick Berthault, and Brian W. Matthews

J. Am. Chem. Soc., **2005**, 127 (33), 11676-11683• DOI: 10.1021/ja053074p • Publication Date (Web): 30 July 2005

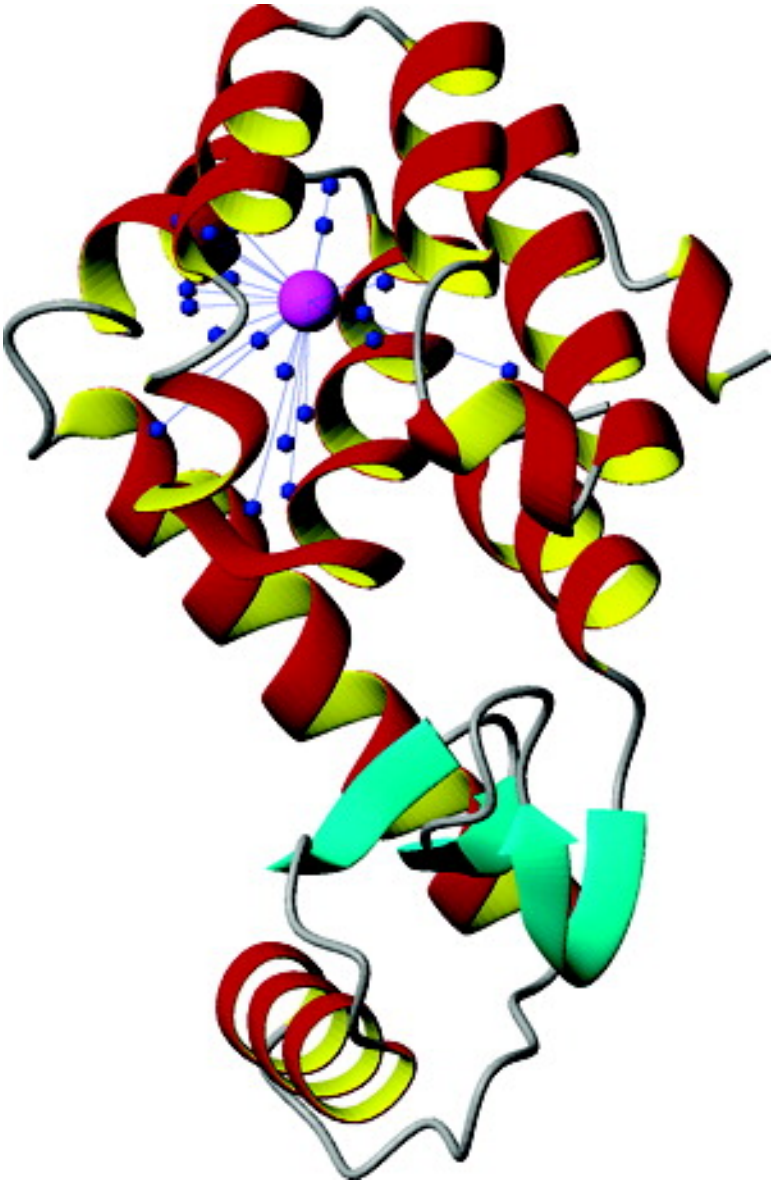

More About This Article

Additional resources and features associated with this article are available within the HTML version:

- Supporting Information
- Links to the 2 articles that cite this article, as of the time of this article download
- Access to high resolution figures
- Links to articles and content related to this article

Journal of the American Chemical Society is published by the American Chemical Society. 1155 Sixteenth Street N.W., Washington, DC 20036

J|A|C|S
ARTICLES
Published on Web 07/30/2005

Dynamics of Xenon Binding Inside the Hydrophobic Cavity of Pseudo-Wild-type Bacteriophage T4 Lysozyme Explored through Xenon-Based NMR Spectroscopy

Hervé Desvaux,*,† Lionel Dubois,† Gaspard Huber,† Michael L. Quillin,‡ Patrick Berthault,† and Brian W. Matthews‡

Contribution from the Laboratoire Structure et Dynamique par Résonance Magnétique, DSM/DRECAM/Service de Chimie Moléculaire, URA CEA/CNRS 331, C.E.A. Saclay, F-91191 Gif sur Yvette, France, and Institute of Molecular Biology, Howard Hughes Medical Institute and Department of Physics, 1229 University of Oregon, Eugene, Oregon 97403-1229

Received May 11, 2005; E-mail: hdesvaux@Cea.fr

Abstract: Wild-type bacteriophage T4 lysozyme contains a hydrophobic cavity with binding properties that have been extensively studied by X-ray crystallography and NMR. In the present study, the monitoring of ^{1}H chemical shift variations under xenon pressure enables the determination of the noble gas binding constant ($K = 60.2\ M^{-1}$). Although the interaction site is highly localized, dipolar cross-relaxation effects between laser-polarized xenon and nearby protons (SPINOE) are rather poor. This is explained by the high value of the xenon−proton dipolar correlation time (0.8 ns), much longer than the previously reported values for xenon in medium-size proteins. This indicates that xenon is highly localized within the protein cavity, as confirmed by the large chemical shift difference between free and bound xenon. The exploitation of the xenon line width variation vs xenon pressure and protein concentration allows the extraction of the exchange correlation time between free and bound xenon. Comparison to the exchange experienced by protein protons indicates that the exchange between the open and closed conformations of T4 lysozyme is not required for xenon binding.

I. Introduction

Although numerous globular proteins have hydrophobic cavities, their biological role and their importance for protein structure and stability are still unclear. Among the few physical methods designed to investigate them at atomic resolution, most studies are based on X-ray diffraction on crystals pressurized by a noble gas, particularly xenon.[1−3] Also various NMR approaches have used small organic compounds,[4] paramagnetic species[5,6] or dissolved noble gases as probes.[7−12] Recently a strategy combining (i) xenon NMR and analysis of the protein resonances in experiments using variable protein and xenon concentrations and (ii) cross-relaxation from laser-polarized xenon to protein protons was shown to allow a detailed characterization of the interaction.[13] The xenon location, its dynamic behavior inside the cavity, and the thermodynamics of the interaction could be determined by this approach.

To compare the X-ray crystallographic and NMR approaches for the study of hydrophobic molecular regions, bacteriophage T4 lysozyme seems a promising choice. In the absence of ligand, this two-domain protein[14,15] exists in two equally populated conformations in solution.[16] The closed form, which is the one found in many X-ray crystal forms,[17] exhibits two buried cavities. The recombinant cysteine-free pseudo-wild-type protein (WT*, C54T/C97A) has been shown to present the same dynamics and the same structure as this wild-type protein.[18] The volume of the largest cavity of the WT* protein, as determined by X-ray crystallography, corresponds fairly well to the xenon atomic volume, and indeed noble gases, such as xenon or argon, are found inside this cavity.[19] On the other hand, the second

† DSM/DRECAM/Service de Chimie Moléculaire.
‡ Howard Hughes Medical Institute and Department of Physics.

(1) Schoenborn, B. P. *Nature* **1965**, *208*, 760.
(2) Prangé, T.; Schiltz, M.; Pernot, L.; Colloc'h, N.; Longhi, S.; Bourguet, W.; Fourme, R. *Proteins: Struct., Funct., Genet.* **1998**, *30*, 61.
(3) Schiltz, M.; Fourme, R.; Prangé, T. *Methods Enzymol.* **2003**, *374*, 83.
(4) Otting, G.; Liepinsh, E.; Halle, B.; Frey, U. *Nat. Struct. Biol.* **1997**, *4*, 396.
(5) Teng, C.-L.; Bryant, R. G. *J. Am. Chem. Soc.* **2000**, *122*, 2667.
(6) Pintacuda, G.; Otting, G. *J. Am. Chem. Soc.* **2002**, *124*, 372.
(7) Rubin, S. M.; Spence, M. M.; Dimitrov, I. E.; Ruiz, E. J.; Pines, A.; Wemmer, D. E. *J. Am. Chem. Soc.* **2001**, *123*, 8616.
(8) Landon, C.; Berthault, P.; Vovelle, F.; Desvaux, H. *Protein Sci.* **2001**, *10*, 762.
(9) Locci, E.; Dehouck, Y.; Casu, M.; Saba, G.; Lai, A.; Lühmer, M.; Reisse, J.; Bartik, K. *J. Magn. Reson.* **2001**, *150*, 167.
(10) Rubin, S. M.; Lee, S.-Y.; Ruiz, E. J.; Pines, A.; Wemmer, D. E. *J. Mol. Biol.* **2002**, *322*, 425.
(11) Gröger, C.; Möglich, A.; Pons, M.; Koch, B.; Hengstenberg, W.; Kalbitzer, H. R.; Brunner, E. *J. Am. Chem. Soc.* **2003**, *125*, 8726.
(12) Corda, M.; Era, B.; Fais, A.; Casu, M. *Biochim. Biophys. Acta* **2004**, *1674*, 182.
(13) Dubois, L.; Da Silva, P.; Landon, C.; Huber, J. G.; Ponchet, M.; Vovelle, F.; Berthault, P.; Desvaux, H. *J. Am. Chem. Soc.* **2004**, *126*, 15738.
(14) Eriksson, A. E.; Baase, W. A.; Zhang, X. J.; Heinz, D. W.; Blaber, M.; Balwin, E. P.; Matthews, B. W. *Science* **1992**, *255*, 178.
(15) Llinás, M.; Gillespie, B.; Dahlquist, F. W.; Marqusee, S. *Nat. Struct. Biol.* **1999**, *6*, 1072.
(16) Goto, N. K.; Skrynnikov, N. R.; Dahlquist, F. W.; Kay, L. E. *J. Mol. Biol.* **2001**, *308*, 745.
(17) Zhang, X.-J.; Wozniak, J. A.; Matthews, B. W. *J. Mol. Biol.* **1995**, *250*, 527.
(18) Nicholson, H.; Anderson, D. E.; Dao-Pin, S.; Matthews, B. W. *Biochemistry* **1991**, *30*, 9816.

10.1021/ja053074p CCC: $30.25

cavity is too small to accommodate xenon. The effect of buried cavities on the stability of the protein has been explored by site-directed mutagenesis.[14] The affinity of various noble gases for the resulting artificial cavities of different sizes was also studied.[17,19] It has also been shown that different mutations can change the interdomain orientation, the average protein conformation being more closed or more open than WT*.[16] Among all mutants, the L99A mutant has been studied most extensively.[19−25] This mutation increases the volume of the largest cavity which can then accommodate up to two xenon atoms[19] and also organic compounds.[25] The most stable conformation of this mutant in solution corresponds to the closed form.[22] In this conformation the cavity is fully buried, and at least for organic compounds, their access to the cavity is related to the exchange between the open and closed conformations.[20,23]

The present NMR study focuses on WT* T4 lysozyme and its interaction with xenon. Although the binding constant evaluated through proton chemical shift mapping is far from negligible, SPINOE experiments evidencing through-space proximities between laser-polarized xenon and protein protons give only poor results. Indeed the proton signal enhancement obtained by these experiments is small compared to that for other proteins. This seems to result from the small size of the cavity, which reduces the volume available to xenon. This is confirmed by xenon longitudinal self-relaxation measurement as a function of the static magnetic fields and is substantiated by the large xenon chemical shift variation (>30 ppm) between free and bound xenon. Finally from the study of the xenon line width as a function of the gas pressure and protein concentration, an exchange rate is extracted. This exchange is much faster than that experienced by the Me_{δ_1} of Leu 121, as determined by off-resonance self-relaxation measurements. This indicates that the binding of xenon inside this buried cavity is not necessarily associated with the exchange between the open and closed conformations of the protein.

II. Material and Methods

A. General NMR Experiments. WT* T4 lysozyme was expressed in *Escherichia coli* and purified as previously described.[26] NMR experiments were performed at 293 K either using D_2O as solvent (the protein sample was previously lyophilized) or in H_2O:D_2O (90:10). The solutions contained 0.55 M NaCl, 0.1 M sodium phosphate, pH = 6.5.

Natural abundance xenon from Air Liquide was used for NMR experiments under controlled xenon pressure, while xenon enriched in isotope 129 from Chemgas was used for optical pumping experiments.

NMR spectra were acquired on Bruker DRX500, DRX600, and DRX800 as well as on a Tecmag DSpect spectrometer for which the proton resonance frequency is 200 MHz. The 500 and 600 MHz spectrometers were equipped with broadband inverse probeheads while the 800 MHz spectrometer was equipped with a triple resonance cryoprobe. Processing of the NMR spectra was performed either using the XWINNMR and NT-NMR software or using Sparky[27] when peak assignments or monitoring of the chemical shift variations was needed. The NMR signal assignment was deduced from the published partial assignment tables (mainly backbone signals[28] and hydrophobic side chains of the L99A mutant[24]). The absence of labeling of our samples and the intense spectral overlap in the aliphatic region prevented us fully completing the assignment based only on NOESY- and TOCSY-type experiments.

The monitoring of the proton chemical shift variations under xenon pressure was deduced from a series of 11 NOESY spectra acquired at 800 MHz, with static pressures of xenon above the 0.7 mM protein solution ranging from 0 to 6 atm. Using the large number of $^1H-^1H$ cross-relaxation peaks, the resonance frequency of each proton experiencing a chemical shift variation can be precisely determined.

The determination of the exchange correlation times τ_{ex} and τ'_{ex} experienced by methyl protons δ_1 of Leu 121 was performed by acquiring, at 800 MHz, a series of 192 one-dimensional (1D) proton off-resonance ROESY spectra on a xenon pressurized sample and a series of 144 1D spectra on a degassed sample.[29,30] These series were composed of eight mixing times ranging from 10 to 60 ms and 24 rf amplitudes ranging between 0.37 and 5.5 kHz for the pressurized sample and 18 rf amplitudes between 0.37 and 4.1 kHz for the degassed one. These amplitudes were carefully determined using a nutation experiment,[31] while the off-resonance ROESY angle θ between the static and the effective fields in the rotating frame was 35.3° for the considered protons. The selective excitation was obtained by an excitation sculpting scheme,[32] the soft inversion pulse being a Gaussian cascade of the Q3 type,[33] of length 25 ms.

During all fitting procedures, the uncertainties on the extracted parameters were computed using experimental estimated errors. Since systematic biases were poorly defined, in the case of Figures 2 and 5A and to illustrate the validity of the derived conclusions, we have represented curves using limit parameter values, i.e., with values much larger and much smaller than those corresponding to the best-fit theoretical ones and the associated errors.

All the figures displaying protein T4 lysozyme structures have been drawn in MolMol 2K.2,[34] using the atom coordinates deposited at the Protein Data Bank, code: 1C6T.[19]

B. Laser-Polarized Xenon. Xenon was polarized by spin-exchange[35] using the apparatus described in ref 36. For the present experiments, protocols similar to those described in ref 8 were used. Typically the gaseous xenon was polarized at a level of about 25%, and the pressure above the solution after xenon addition was between 0.5 and 3 atm.

For the detection of dipolar cross-relaxation between xenon and nearby protons, the SPINOE pulse sequence described in ref 36 was used. It consisted of a difference spectroscopy of the built-up proton magnetization in the presence of positively or negatively polarized xenon magnetization. These build-ups started from a saturated proton magnetization obtained by a series of 32 proton 90° hard pulses, each followed by a pulsed field gradient of random amplitude. Very short recycling delays (30 ms + 110 ms of acquisition) were used. Each

(19) Quillin, M. L.; Breyer, W. A.; Griswold, I. J.; Matthews, B. W. *J. Mol. Biol.* **2000**, *302*, 955.
(20) Feher, V. A.; Baldwin, E. P.; Dahlquist, F. W. *Nat. Struct. Biol.* **1996**, *3*, 516.
(21) Mann, G.; Hermans, J. *J. Mol. Biol.* **2000**, *302*, 979.
(22) Mulder, F. A. A.; Hon, B.; Muhandiram, D. R.; Dahlquist, F. W.; Kay, L. E. *Biochemistry* **2000**, *39*, 12614.
(23) Mulder, F. A. A.; Mittermaier, A.; Hon, B.; Dahlquist, F. W.; Kay, L. E. *Nat. Struct. Biol.* **2001**, *8*, 932.
(24) Mulder, F. A. A.; Hon, B.; Mittermaier, A.; Dahlquist, F. W.; Kay, L. E. *J. Am. Chem. Soc.* **2002**, *124*, 1443.
(25) Eriksson, A. E.; Baase, W. A.; Wozniak, J. A.; Matthews, B. W. *Nature* **1992**, *355*, 371.
(26) Matsumura, M.; Becktel, W. J.; Levitt, M.; Matthews, B. W. *Proc. Natl. Acad. Sci. U.S.A.* **1989**, *86*, 6562.
(27) Goddard, T. D.; Kneller, D. G. *SPARKY 3*, University of California, San Francisco.
(28) McIntosh, L. P.; Wand, A. J.; Lowry, D. F.; Redfield, A. G.; Dahlquist, F. W. *Biochemistry* **1990**, *29*, 6341.
(29) Desvaux, H.; Birlirakis, N.; Wary, C.; Berthault, P. *Mol. Phys.* **1995**, *86*, 1059.
(30) Desvaux, H.; Berthault, P. *Prog. Nucl. Magn. Reson. Spectrosc.* **1999**, *35*, 295.
(31) Guenneugues, M.; Berthault, P.; Desvaux, H. *J. Magn. Reson.* **1999**, *136*, 118.
(32) Stott, K.; Stonehouse, J.; Keeler, J.; Hwang, T.-L.; Shaka, A. J. *J. Am. Chem. Soc.* **1995**, *117*, 4199.
(33) Emsley, L.; Bodenhausen, G. *J. Magn. Reson.* **1992**, *97*, 135.
(34) Koradi, R.; Billeter, M.; Wüthrich, K. *J. Mol. Graphics* **1996**, *14*, 51.
(35) Walker, T. G.; Happer, W. *Rev. Mod. Phys.* **1997**, *69*, 629.
(36) Desvaux, H.; Gautier, T.; Le Goff, G.; Pétro, M.; Berthault, P. *Eur. Phys. J. D* **2000**, *12*, 289.

SPINOE experiment, acquired in about 2 min, consisted of 32 ^{1}H spectra for a mixing time of 600 ms. The spectra were added in the processing step, thus enabling optimization of the number of accumulations. Before each SPINOE experiment, the NMR tube was vigorously shaken to refresh dissolved laser-polarized xenon by exchange from the gas phase. After reinsertion of the tube into the magnet, the xenon magnetization of positive spin temperature was monitored by a small read pulse (about 2°) and the SPINOE experiment, which was preceded by four dummy scans, was acquired.

To measure the xenon longitudinal self-relaxation rates, a known amount of polarized xenon was added to the degassed protein solution. This quantity was further checked after the NMR experiment by expansion of the gas located above the frozen solution in a volume equipped with a pressure gauge. After adding the xenon and shaking the NMR sample, the experiments were begun. They consisted of a small xenon flip angle ϑ (< 5°) followed by the acquisition of the xenon NMR signal. Typically 32 spectra were acquired with an interscan delay optimized according to the xenon self-relaxation times (between 4 and 30 s). To correct the xenon signal decay for the effect of the flip angle ϑ and to determine the exact xenon longitudinal self-relaxation time T_1, a series of xenon NMR spectra with short interscan delay (<1 s) and the same flip angle ϑ was acquired. The exploitation of the latter allowed the extraction of the xenon signal decrease factor (cos ϑ) for each acquisition.[37] Using this value and a home-written C program, the xenon decay curves as a function of time t_n were fitted to the function $\cos^{n-1}\vartheta \exp(-t_n/T_1)$ with n the spectrum number. The xenon self-relaxation times T_1 could thus be determined.

III. Results and Discussion

A. Protein Chemical Shifts. WT* T4 lysozyme exists in solution with two conformations in fast exchange (on the chemical shift time scale) with almost the same population.[16] Due to this equilibrium, large variations of the protein chemical shifts may be expected when xenon binds inside the hydrophobic cavity of the closed conformation, since the ratio of the two conformers can change. A series of 11 NOESY spectra was then acquired on a 0.7 mM protein solution dissolved in H_2O. The static xenon pressure above the solution was varied from 0 to 6 atm. By comparing the cross-peak positions on the 2D NOESY maps within the series, the chemical shifts of 210 protons were monitored as a function of the xenon pressure. This number was reduced to 76 when only variations larger than 5 times the uncertainty in the peak frequency determination were kept.

All chemical shift variations, $\Delta\delta$, under xenon pressure can be described by a specific model of interaction of stoichiometry 1:1 with a binding constant K:

$$\Delta\delta = \frac{\Delta\delta_{max} K[Xe]}{1 + K[Xe]} \quad (1)$$

with [Xe] representing the xenon concentration in solution, and $\Delta\delta_{max}$ the difference of proton chemical shift between the unliganded protein and the complex. For each proton, the binding constant extracted by least-squares fitting falls in the range 50−70 M^{-1}. The 76 significant chemical shift variations were then fitted together against eq 1 to determine the global best-fit K value (Figure 1). A binding constant of 60.2 ± 0.2 M^{-1} was determined, assuming a xenon solubility of 4.5mM/atm (reduced $\chi^2 = 0.75$). This K value was used in the following calculations. At a level of confidence of 99% the K value is between 55 and 64 M^{-1}. $\Delta\delta_{max}$ values range between 0.128 and −0.159 ppm, revealing nonnegligible proton chemical shift variations when xenon is bound to the protein.

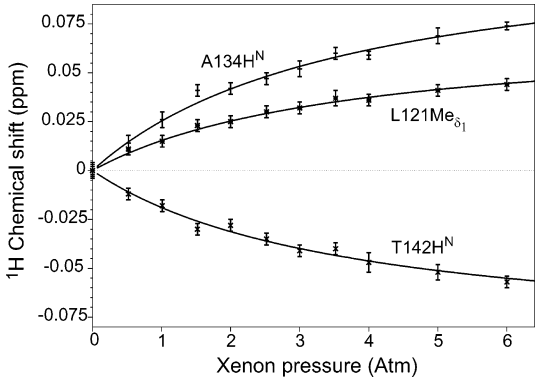

Figure 1. Examples of protein proton chemical shift variations under xenon pressure. The best-fit theoretical curves to eq 1 (assuming a specific model with a binding constant of 60.2 M^{-1}) are superimposed.

Fifty-one out the 76 protons experiencing significant chemical shift variations have been assigned (see Supporting Information). Most of them correspond to protons in the vicinity of the protein cavity. However, as for the case of the L99A mutant,[22] protons close to the hinge of the protein and associated with the conformational exchange between the open and closed conformations of the protein are detected (e.g. the protons of the Phe 104[17]). This observation indicates that, as for the L99A mutant, the binding of xenon inside the WT* cavity displaces the equilibrium toward the closed conformation.

Comparison of the binding constant K with other protein−xenon binding constants reveals that the affinity of WT* lysozyme for xenon is in the medium range. K is smaller than that for the first site of metmyoglobin (190 M^{-1}) but larger than that for the second site (10 M^{-1}).[38] K is close to that of xenon−LTP1 complexes,[13,39] although their cavities are of much larger volume. As a consequence, the contributions of entropy and enthalpy to the free energy associated with xenon binding in LTP1 and T4 lysozyme should be very different. Among the different T4 lysozyme mutants, the affinity of xenon for WT* is smaller than that for the main cavity of the L99A mutant (90 M^{-1}) but similar to that for its second site (50 M^{-1}).[10] These results on the different affinities of xenon to cavities of T4 lysozyme mutants agree with the occupancies estimated from crystallographic refinement of X-ray diffraction under 8 atm of xenon.[19]

B. SPINOE Experiment. The presence of highly polarized xenon induces a variation of the nuclear polarization of the neighboring protons through dipolar cross-relaxation. The so-called SPINOE[40] is detectable only if the proton self-relaxation time is very long and if there is a specific interaction between xenon and the molecule.[41] This direct approach permits possible determination of the xenon interaction sites and avoids indirect

(37) Gerhard, P.; Koch, M.; Jänsch, H. J. *C. R. Physique* **2004**, *5*, 297.

(38) Tilton, R. F.; Kuntz, I. D. J. *Biochemistry* **1982**, *21*, 6850.
(39) Dubois, L.; Parrès, S.; Huber, J. G.; Berthault, P.; Desvaux, H. *J. Phys. Chem. B* **2004**, *108*, 767.
(40) Navon, G.; Song, Y.-Q.; Rõõm, T.; Appelt, S.; Taylor, R. E.; Pines, A. *Science* **1996**, *271*, 1848.
(41) Dubois, L.; Berthault, P.; Huber, J. G.; Desvaux, H. *C. R. Physique* **2004**, *5*, 305.

effects which may be present in the chemical shift mapping approach.[13] This experiment has consequently been applied to localize xenon inside WT* T4 lysozyme. However, although several attempts have been made to optimize the polarization transfer, all acquired SPINOE spectra show a low signal-to-noise ratio (see Supporting Information). According to all tests performed on the xenon magnetization and polarization, on the stability of the SPINOE experiments, and on the xenon longitudinal self-relaxation time T_1 in the high field spectrometer, the only reasonable explanation resides in the particular dynamics of the xenon−T4 lysozyme complex which slows the polarization transfer process and reduces the absolute xenon magnetization at the beginning of the SPINOE experiment. Indeed it has already been shown through simple considerations of the dependence of the dipolar relaxation rates on the spectral density functions that the SPINOE efficiency is largely reduced for long correlation times and therefore for xenon buried in the cavity of a protein.[39,41,42]

The direct assignment of the obtained SPINOE spectra is difficult due to their low signal-to-noise ratio and the strong ^{1}H signal overlaps on a 1D spectrum of a 164 amino acid protein. We have consequently assigned them by an iterative procedure based on the unambiguous peaks and the proximity of the associated nuclei to other protons. By using this procedure, 19 protons have been found to interact with xenon (See Supporting Information). They are either protons at the surface of the protein cavity or protons near those experiencing direct SPINOE, due to ^{1}H−^{1}H spin-diffusion process which is very efficient for such a large protein. The tentative assignments of nine other resonances based on our partial chemical shift table were never substantiated by the detection of other nearby protons. In particular there is no indication of a possible binding site for xenon different from the main T4 lysozyme cavity. As a consequence, based on the SPINOE signals, it is clear that xenon only probes the main cavity of T4 lysozyme and is consequently located inside. This result corresponds to the first confirmation by SPINOE-based NMR of a location found by X-ray crystallography.[19] It is also the first observation of selective SPINOE on a protein composed of more than 100 amino acids.

C. Xenon Longitudinal Self-Relaxation. The xenon dynamics inside the T4 lysozyme cavity can be explored using the same method as that used for wheat LTP1.[39] A series of xenon longitudinal self-relaxation time measurements was performed at three static magnetic fields (4.7, 11.7, and 14.1 T) and for various experimental conditions. For a given magnetic field, up to 10 combinations of protein and xenon concentrations were used. For each combination, the decay of the laser-polarized xenon signal as a function of time was monitored, and the xenon longitudinal self-relaxation time T_1 was determined. Surprisingly, even with a protein concentration of 1.36 mM and xenon pressure of 1.1 atm, the extracted xenon T_1 are still long (>100 s). This range of T_1 values is, a priori, well adapted to the experimental implementation of SPINOE. Too-short xenon T_1 values in the spectrometer magnetic field cannot consequently explain the low ^{1}H signal enhancements observed in SPINOE spectra.

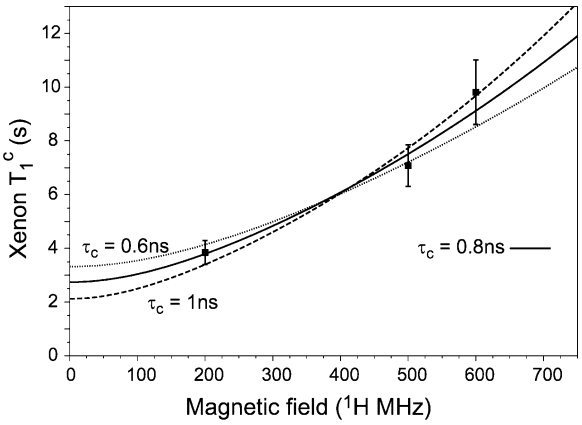

Figure 2. Variation of the longitudinal self-relaxation time T_1^c of bound xenon as a function of the static magnetic field value. The best-fit theoretical curve (solid line) assuming dipolar relaxation and Lorentzian spectral density function is superimposed. The extracted correlation time is equal to 0.8 ns. Two limit values for the correlation time (τ_c = 1 ns, dashed line) and (τ_c = 0.6 ns, dotted line) are also represented.

Considering that the measured xenon self-relaxation rate $1/T_1$ is a weighted average of that of free xenon ($1/T_1^f$) and of that of bound xenon ($1/T_1^c$):

$$\frac{1}{T_1} = \frac{f}{T_1^c} + \frac{1-f}{T_1^f} \tag{2}$$

f is the fraction of bound xenon which can be computed using the binding constant value K, the protein concentration, and the xenon pressure. For each magnetic field, using the different experimental conditions (protein concentrations and xenon pressures), the xenon self-relaxation time T_1^c was extracted. In Figure 2, the variation of the self-relaxation time of bound xenon T_1^c as a function of the static magnetic field is reported.

In contrast to the case of wheat LTP1,[39] for WT* T4 lysozyme a strong field dependence of the xenon T_1^c is observed. Moreover the T_1^c values are much shorter than those obtained for the LTP1 proteins.[13,39]

To better quantify the dynamic behavior we assume (i) that the xenon relaxation is only due to dipolar interaction with protons and (ii) that all xenon−proton dipolar spectral densities $J_n(\omega)$ can be represented by a Lorentzian function characterized by the same correlation time τ_c:

$$J_n(\omega) = \frac{3}{10}\frac{\gamma_H^2\gamma_{Xe}^2\hbar^2}{r_{H_nXe}^6}\frac{\tau_c}{1+\omega^2\tau_c^2} \tag{3}$$

Using this model, the correlation time τ_c can be determined from the experimental T_1^c value by nonlinear least-squares fitting. The xenon longitudinal self-relaxation time functions computed with this model using the best-fit τ_c value and limits of acceptable τ_c values are superimposed on the experimental T_1^c in Figure 2. The best-fit correlation time is 0.8 ns. This value is significantly larger than that obtained for wheat LTP1 (0.4 ns).[39] Investigation of possible chemical shift anisotropy (CSA) contribution to xenon relaxation reveals that it should be small. Indeed a large CSA associated with a correlation time in the nanosecond range would induce a decrease of the xenon T_1 at high field, whereas we observe an increase.

(42) Lühmer, M.; Goodson, B. M.; Song, Y.-Q.; Laws, D. D.; Kaiser, L.; Cyrier, M. C.; Pines, A. *J. Am. Chem. Soc.* **1999**, *121*, 3502.

The net effect of this longer correlation time on SPINOE is a decrease of the xenon−proton cross-relaxation rate to direct relaxation rate ratio by a factor about 2. Moreover the shorter xenon T_1 at low field induces an efficient xenon relaxation during the shaking of the NMR tube in the fringe field of the NMR magnet, shaking needed to renew dissolved laser-polarized xenon before starting any SPINOE experiment. As a consequence and as noted, the absolute xenon magnetization cannot be as large in the case of T4 lysozyme as values obtained for tobacco LTP1[13] or β-cryptogein.[43]

From a biophysical point of view, this much longer correlation time reveals that the mobility of xenon inside the cavity of T4 lysozyme is much more restricted than in wheat LTP1, which is expected as the latter has a much larger cavity volume (>300 Å^3). On the basis of the X-ray structure of the complex (PDB code: 1C6T, ref 19), this tendency is expected since the cavity of the WT* T4 lysozyme is slightly enlarged during xenon binding.[19] Moreover the crystallographic *B*-factor for xenon is similar to that of the surrounding atoms, while for other mutants with larger hydrophobic cavities the xenon *B*-factor can be significantly larger. On the other hand the extracted correlation time is still much shorter than the overall protein correlation time, about 9.8 ns,[22] revealing that even in a cavity of volume similar to xenon, efficient dynamics must be present to average the dipolar interactions. This implies substantial dynamics of the amino acid side chains bordering the cavity. Investigation as to whether this side-chain dynamics is reduced when xenon is bound would require protein isotope (^{2}H, ^{13}C) labeling.[22,44]

D. Xenon Chemical Shift Variation. Variation of the xenon chemical shift as a function of gas pressure and protein concentration has been reported for many proteins.[7−13] It is a classical procedure for exploring the affinity between the noble gas and a protein. This effect results from specific and nonspecific interactions,[9,45] the latter being more related to the exploration of the protein surface sites by xenon. At constant protein concentration and a small range of xenon concentrations, the first effect is consequently predominant. Figure 3 illustrates the xenon chemical shift variations for a series of experiments acquired at 11.7 and 14.1 T. In the range of xenon pressures used, the observed chemical shift variations $\Delta\delta_{Xe}$ at constant protein concentration are assumed to depend only on the binding effect:

$$\Delta\delta_{Xe} = f\Delta\delta_s + \Delta\delta_{ns} \quad (4)$$

where $\Delta\delta$ is the variation of xenon chemical shift between free and bound xenon due to specific interaction and $\Delta\delta_{ns}$ is the nonspecific contribution which is protein-concentration dependent. We can notice that, as in all studied proteins except horse and sperm whale myoglobin,[10,38] the chemical shift value of bound xenon is larger than that of free xenon.

From the five sets of variations acquired under the same conditions (same day in the same static magnetic field) $\Delta\delta_s$ is determined by least-squares fitting using the binding constant *K* previously determined. The best-fit value $\Delta\delta_s = 32.4 \pm 2.0$ ppm (reduced $\chi^2 = 0.964$) is large with respect to values

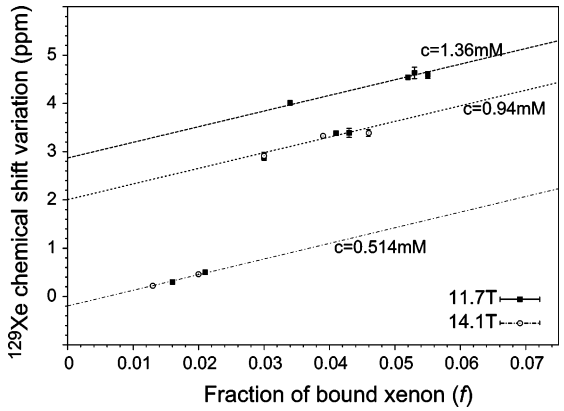

Figure 3. Variation of the xenon chemical shift as a function of the fraction of bound xenon. Two static magnetic fields are considered (filled symbols for 11.7 T and open symbols for 14.1 T), and three different protein concentrations. The slopes of all straight lines are identical and allow the determination of $\Delta\delta_s$, found equal to 32.4 ± 2.0 ppm (eq 4). The experiments have not been acquired in conditions such that the nonspecific contribution $\Delta\delta_{ns}$ can be extracted. Thus, the relative vertical position of the different lines has no physical meaning.

reported thus far for other protein sites. Nevertheless, for these proteins the cavity volume is much larger than the xenon van der Waals volume. The only similar condition corresponds to xenon inside the second small cavity of L99A mutant of T4 lysozyme.[10] In the latter case, Rubin et al. also reported a large xenon chemical shift variation equal to 30 ± 10 ppm.[10] They concluded, on the basis of the study of different proteins, that the xenon chemical shift increases when the protein cavity size decreases. This behavior differs completely from the case of cryptophane cavities for which the bound xenon chemical shift is smaller than that of dissolved xenon and decreases with the cavity size.[46,47] As a consequence, the xenon chemical shift associated with small hydrophobic protein cavities seems to result from the strong interactions between xenon and the nearby amino acid side chains, in this case mainly methyl groups.

E. Xenon Resonance Line Width. The xenon spectra reveal large changes in line width as a function of the gas and WT* T4 lysozyme protein concentrations (Figure 4). Since laser-polarized xenon allows accurate NMR measurements, the xenon resonance line width has never been exploited, although different behaviors exist. For instance, in the case of LTP1 proteins[8,13] or β cryptogein[43] no significant variation of the xenon resonance line width is observed as a function of the bound xenon fraction. On the other hand, in the case of maltose-binding protein, a significant broadening of the xenon resonance is observed when the protein concentration increases.[10] The case of T4 lysozyme mutants is also interesting, as the xenon line width increases with the reduction of the protein cavity volume.[10]

For WT* T4 lysozyme, the full line widths at middle height $\Delta\nu_{1/2}$ are measured between 40 and 190 Hz at 11.7 T and up to 270 Hz at 14.1 T. These large values and large variations cannot be due to changes in the static magnetic field homogeneity from one experiment to the other, since well-resolved ^{1}H NMR spectra are observed. They must consequently result from particular transverse self-relaxation properties of xenon.

As for xenon longitudinal self-relaxation, it is expected that the transverse self-relaxation rate, $1/T_2 = \pi\Delta\nu_{1/2}$, is a weighted

(43) Berthault, P.; Huber, G.; Ha, P. T.; Dubois, L.; Desvaux, H.; Guittet, E. *ChemBioChem.* **2005**. Manuscript submitted.
(44) Skrynnikov, N. R.; Mulder, F. A. A.; Hon, B.; Dahlquist, F. W.; Kay, L. E. *J. Am. Chem. Soc.* **2001**, *123*, 4556.
(45) Rubin, S. M.; Spence, M. M.; Goodson, B. M.; Wemmer, D. E.; Pines, A. *Proc. Natl. Acad. Sci. U.S.A.* **2000**, *97*, 9472.
(46) Brotin, T.; Dutasta, J.-P. *Eur. J. Org. Chem.* **2003**, 973.
(47) Sears, D. N.; Jameson, C. J. *J. Chem. Phys.* **2003**, *119*, 12231.

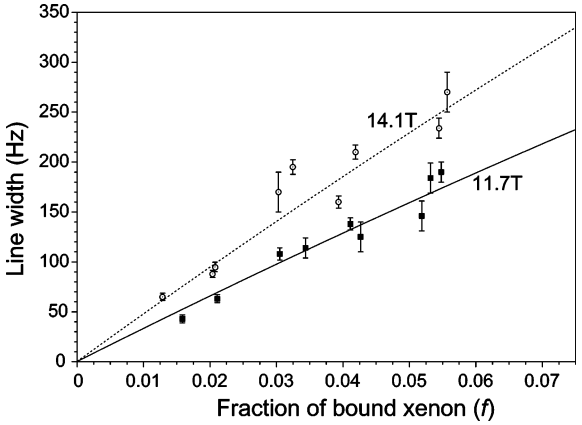

Figure 4. Variation of the xenon line width as a function of the fraction of bound xenon for the two static magnetic fields: 11.7 T (filled symbols) and 14.1 T (open symbols). The best-fit theoretical curves to eq 5 are superimposed. Using $\Delta\delta_s = 32.4$ ppm (Figure 3) and eq 5 the extracted exchange correlation time τ_e is equal to 13 ± 4 μs.

average of the free $1/T_2^f$ and bound xenon relaxation rates $1/T_2^c$, due to modulation of the interactions on the nanosecond time scale. Nevertheless the presence of a chemical shift difference between free and bound xenon leads to a supplementary contribution:

$$\frac{1}{T_2} = \frac{f}{T_2^c} + \frac{1-f}{T_2^f} + f(1-f)(\gamma_{Xe}\Delta\delta_s B_0)^2\tau_e \qquad (5)$$

where B_0 is the static magnetic field and τ_e is the exchange correlation time associated with the exchange between free and bound xenon.

Using the classical expression for transverse dipolar self-relaxation, the correlation time τ_c and distances extracted from the xenon T_1 dependence on magnetic field, the contribution $1/T_2^c$ can be computed. The T_2^c values are on the order of 3.2 s at 11.7 T and 3.6 s at 14.1 T. The broadening of the line cannot consequently be explained by this contribution. On the other hand, due to the large change of xenon chemical shift in the present complex, the last term of eq 5 can lead to an important contribution and can thus explain the observed line broadening. By least-squares fitting the observed xenon resonance line width to eq 5, the exchange correlation time τ_e value at 293 K is determined. It is equal to 13 ± 4 μs. The best-fit theoretical curves are superimposed on the experimental line widths in Figure 4. The agreement for the two data sets reveals the net existence of a B_0^2 dependence of the xenon line width.

F. Exchange Rate between the Free T4 Lysozyme and Its Complex with Xenon. The exchange correlation time of xenon τ_e appears to be very short. This means that even in a buried protein cavity such as that of T4 lysozyme, xenon is able to get inside on a microsecond time scale. There is no report of the exchange rate of xenon between free and bound states in T4 lysozyme mutants. However, the dynamics of the L99A mutant of T4 lysozyme was explored by ^{15}N and ^{2}H relaxation studies. The extracted exchange correlation time between the open and closed conformations was found equal to about 625 μs.[22] Assuming that xenon enters the cavity when the protein is in its open conformation, as is the case for the binding of organic compounds,[20,23] then the xenon exchange correlation time for this protein is expected to be on the order of 625 μs. This value obviously differs from our finding. This exchange between the

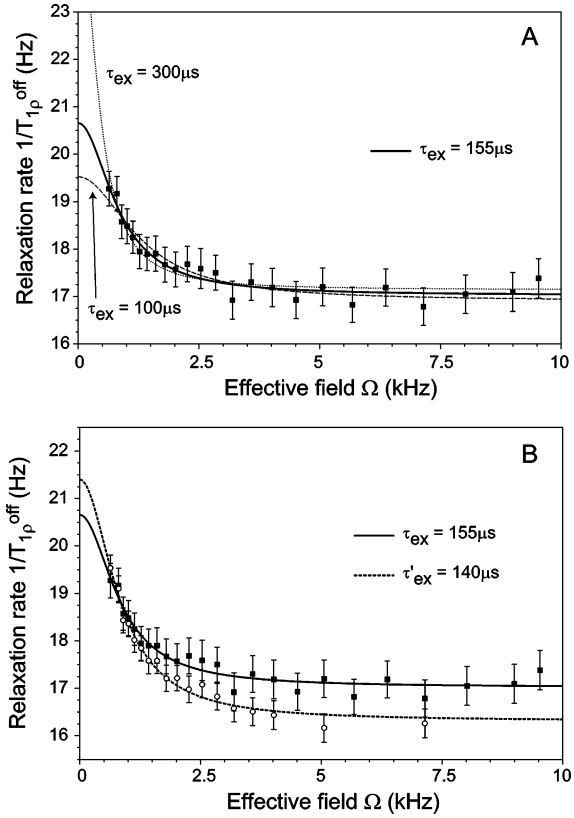

Figure 5. Off-resonance self-relaxation rates $1/T_{1\rho}^{off}$ of Me_{δ_1} of Leu 121 measured at 800 MHz for an angle $\theta = 35.3°$, as a function of the effective field amplitude Ω. (A) Decay rates measured on a sample pressurized with 3.7 atm of xenon. The best-fit theoretical curve (solid line) to eq 6 is superimposed. The extracted exchange correlation time τ_{ex} is equal to 155 $\pm$ 25 μs. The curves corresponding to τ_{ex} values of 100 and 300 μs are also shown. (B) Superimposition of the decay rates and best-fit theoretical curves for the pressurized sample (closed symbols, same as A) and for the degassed sample (open circles). For this last case, the extracted exchange correlation time τ'_{ex} is equal to 140 ± 15 μs.

open and closed conformations has not yet been characterized in the case of WT* T4 lysozyme. Goto et al. only report that it should be faster than 6 kHz, putting an upper limit for the exchange correlation time at about 170 μs.[16]

This exchange has been characterized by measurement of the ^{1}H relaxation rates of the isolated methyl δ_1 resonance of L121 as a function of the applied magnetic field. This signal experiences significant chemical shift variation under xenon binding ($\Delta\delta_{max} = 0.072$ ppm, Figure 1). A 3.7 atm xenon pressure is applied to the NMR tube to obtain a condition such that there is 50% of complex and 50% of xenon-free protein, based on the obtained K value. The rf irradiation is applied off-resonance, defining an angle θ between the static and the effective fields in the rotating frame equal to 35.3° for which the proton−proton dipolar cross-relaxation rates vanish for large molecules. In Figure 5A, the decay rates, measured at 800 MHz, are reported as a function of the effective field values Ω. It clearly appears that the observed rate $1/T_{1\rho}^{off}$ depends on the rf irradiation strength $\omega_1 = \Omega \sin\theta$. The decay rate is:[29,30]

$$\frac{1}{T_{1\rho}^{off}} = \left.\frac{1}{T_{1\rho}^{off}}\right|_{fast} + \sin^2\theta\, J_{ex}(\Omega) \qquad (6)$$

where the first term, $1/T_{1\rho}^{off}|_{fast}$, corresponds to the contribution of the fast dynamics (correlation times in the nanosecond time

scale) to relaxation. The second contribution is due to the fast chemical exchange experienced by the proton, with an exchange spectral density $J_{ex}(\Omega)$. Assuming a simple two-site model for the chemical exchange allows the computation of $J_{ex}(\Omega)$:

$$J_{ex}(\Omega) = f(1-f)(\gamma_H B_0 \Delta\delta_{complex})^2 \frac{\tau_{ex}}{1+\Omega^2\tau_{ex}^2} \qquad (7)$$

where $\Delta\delta_{complex}$ is the ^{1}H chemical shift difference between the free and xenon-bound protein and τ_{ex} is the exchange correlation time.

In Figure 5A the best-fit theoretical curve to eq 6 is superimposed on the experimental decay rates $1/T_{1\rho}^{off}$. The best-fit correlation time τ_{ex} is equal to 155 ± 25 μs, in agreement with predictions of Goto et al.[16] On a qualitative point of view, from the experimental rates, the exchange correlation time ranges between 100 and 300 μs and a value on the order of 13 μs can definitively be ruled out.

In Figure 5B, we have superimposed on the previous decay rates, those determined on the degassed sample. The observed rate $1/T_{1\rho}^{off}$ also depends on the effective field strength Ω. The extracted exchange correlation time τ'_{ex} is equal to 140 ± 15 μs, and is consequently similar to that obtained in the presence of xenon. The term proportional to the chemical shift difference $\sqrt{f(1-f)}\Delta\delta_{complex}$ is equal to 0.144 ± 0.003 ppm while it is slightly smaller (0.121 ± 0.003 ppm) for the xenon pressurized sample. We finally note that the limit values for large rf field strengths are smaller for the degassed sample (16.26 ± 0.08 Hz) than for the xenon pressurized one (17.02 ± 0.05 Hz).

G. Discussion on the Rates of Xenon Binding and Protein Conformational Exchange. It is hard to reconcile the two exchange correlation times τ_e and τ_{ex}. The value τ_{ex} found from the analysis of the protein proton resonances results from an exchange spectral density function. As it is sampled by more points, it seems consequently of higher confidence than the τ_e value determined from the xenon resonance line width. On the other hand, τ_e cannot be underestimated by a factor of 12. Indeed the behavior of the xenon resonance line width as a function of the bound xenon fraction f effectively depends on the square of the magnetic field, according to the measurements made at 11.7 and 14.1 T (Figure 4). It should consequently represent either a chemical exchange effect or a chemical shift anisotropy contribution to relaxation. But the observed contribution is much too large to agree with a correlation time in the nanosecond time scale. Indeed the model based on chemical shift anisotropy contribution leads to unrealistic CSA values: larger than 2900 ppm with a correlation time equal to that of the protein (9.8 ns) and 10000 ppm using the value of 0.8 ns derived from the T_1 measurement. Moreover the variation of the xenon T_1 as a function of the magnetic field does not at all agree with a large (> 10 ppm) CSA contribution. The observed variation of the xenon resonance line width should consequently result from a chemical exchange effect, and therefore $\Delta\delta_s^2\tau_e$ is correctly estimated from the observed line width variation. Assuming that τ_e is equal to τ_{ex} leads to the conclusion that the chemical shift variation $\Delta\delta_s$ between free and bound xenon is overestimated by a factor about 3.5. This seems unlikely based (i) on the protocol used to extract it (Figure 3) (ii) on the agreement between the value determined here and that observed for xenon inside a cavity of similar size and composition (site 2 of L99A mutant[10]) and (iii) on the observed correlation between the cavity volume and $\Delta\delta_s$.[10]

Finally we can ask if the two methods effectively probe the same phenomena. Indeed the xenon line width analysis samples the process of xenon binding while for the methyl protons of L121, the measurements may also be affected by the exchange between the open and closed conformations of WT* T4 lysozyme. This interpretation is substantiated by the relaxation measurements performed on the degassed sample. Indeed, even without xenon, an open-closed exchange is present with a correlation time τ'_{ex} in agreement with the prediction of Goto et al.[16] If we assume that the two conformations are equally populated in the absence of xenon ($f = 1/2$), the extracted chemical shift difference $\Delta\delta_{complex}$ is equal to 0.073 ppm (Figure 5B). This value can be compared to the chemical shift variation under xenon binding. If the addition of xenon displaces the equilibrium from equally populated open and closed conformations to a fully populated closed conformation, it would result in variation of the proton average chemical shift equal to $\Delta\delta_{complex}/2 = 0.036$ ppm which is clearly different from the observed value ($\Delta\delta_{max} = 0.072$ ppm, Figure 1). As a consequence, the presence of xenon induces a variation of the Me_{δ_1} chemical shift not only due to a change in the populations between the open and closed conformations but also to a direct effect. Me_{δ_1} consequently experiences at least a three-state exchange—two states present in the absence of xenon and at least a third one resulting from the binding of xenon. The signature of the latter exchange on the decay rate curves certainly appears as the difference of $1/T_{1\rho}^{off}$ limit values for large effective fields.

The computation of the spectral density function J_{ex} can be performed using models of exchange more sophisticated than the two-state one.[48] Actually a three-state exchange becomes dependent on two exchange correlation times which are not necessarily directly related to each of the two processes. For instance, consider the following exchange model between the unliganded open conformation, the closed conformation and the closed conformation with xenon inside (Xe@closed):

$$\text{open} \rightleftharpoons \text{closed} \rightleftharpoons \text{Xe@closed} \qquad (8)$$

Denoting τ'_{ex} as the exchange correlation time of the isolated "open ⇌ closed" exchange and τ_e that of the isolated "closed ⇌ Xe@closed" exchange, we can calculate the two eigenvalues of the model (eq 8), using the conditions of the experiments of Figure 5A for the populations:

$$\lambda_\pm = \frac{1}{2}\left(\left(\frac{1}{\tau'_{ex}} + \frac{1}{\tau_e}\right) \pm \sqrt{\left(\frac{1}{\tau'_{ex}} - \frac{1}{\tau_e}\right)^2 + \frac{3}{\tau_e\tau'_{ex}}}\right) \qquad (9)$$

τ'_{ex} and τ_e are experimentally deduced from the protein relaxation measurements in the absence of xenon (Figure 5A) and from the xenon transverse relaxation measurements (Figure 4), respectively. If the shortest correlation time, $1/\lambda_+ \simeq 12$ μs, is still compatible with the measurements, the longest one, $1/\lambda_- \simeq 600$ μs, does not at all agree with them (Figure 5A). The simplest model of exchange (eq 8) can consequently be ruled out.

(48) Wennerström, H. *Mol. Phys.* **1972**, *24*, 69.

In contrast, the triangular model of exchange:

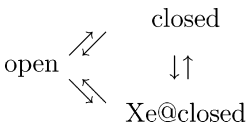

(10)

seems to be in better agreement with the present measurements. Indeed, the longer correlation time can be kept similar in the presence and in the absence of xenon. It would be difficult to push this analysis much further, based on the present relaxation measurements, since while the number of $1/T_{1\rho}^{\text{off}}$ values is large, their limited precision for large effective field strengths prevents the refinement and the discrimination of the models.

Nevertheless, the analysis of the discrepancy between the extracted τ_e and τ_{ex} values indicates that xenon binds inside the T4 lysozyme cavity at a rate higher than that corresponding to the protein conformational exchange. This seems at first sight surprising. However, the fact that xenon is found inside the cavity by X-ray crystallography,[19] with the protein held in its closed conformation, indicates that the protein, even in the crystal, is sufficiently dynamic to enable the access to the cavity through concerted amino acid side-chain motions.

IV. Conclusions

The present NMR study of xenon binding inside a hydrophobic cavity has allowed a comparison with the X-ray crystallographic approach. The two approaches are generally in agreement. First, the affinities determined in solution correlate with the xenon occupancies in crystals. Second, the xenon location is also the same, as checked from the assigned SPINOE peaks. Finally the dynamic properties of xenon on the nanosecond time scale can be compared to the variation in the crystallographic *B*-factors.

From a structural point of view each approach has its own advantages and drawbacks. For example SPINOE techniques were able to locate xenon inside β-cryptogein[43] for which X-ray crystallography under xenon pressure was unsuccessful.[49] In contrast, the SPINOE spectra obtained on WT* T4 lysozyme exhibit poor signal-to-noise ratios, and in this case X-ray analysis of the crystallized protein in the presence of pressurized xenon was better suited for determining the xenon binding site. We have shown that the inefficiency of the SPINOE study results from particular dynamic properties of xenon inside this protein cavity. The most striking result obtained during the present NMR approach deals with the rate of xenon binding. The data indicate that the binding of xenon, in contrast to the binding of small organic compounds, is not correlated with and is much faster (about a factor 12) than the conformational exchange between the open and closed conformations of WT* lysozyme. This first insight on the dynamics of gas binding inside a protein cavity improves the prospects for the quantitative measurement of conformational exchange processes which, to date, have been studied only by computational methods.

Acknowledgment. The French Ministry of Research is acknowledged for financial support (ACI 4103 to H.D.). B.W.M. acknowledges support from the NIH (Grant GM21967). The 800 MHz spectrometer was purchased thanks to financial support from the "Association pour la Recherche contre le Cancer" and the "Conseil Régional d'Ile-de-France".

Supporting Information Available: A table containing the list of atoms experiencing chemical shift variations under xenon pressure; a table giving the list of atoms detected in SPINOE; a figure showing the location on the protein structure of ^{1}H atoms experiencing chemical shift variation under xenon pressure; a SPINOE spectrum acquired on WT* T4 Lysozyme; a figure showing the location on the protein structure of ^{1}H atoms detected by SPINOE. This material is available free of charge via the Internet at http://pubs.acs.org.

JA053074P

(49) Lascombe, M.-B.; Ponchet, M.; Venard, P.; Milat, M.-L.; Blein, J.-P.; Prangé, T. *Acta Crystallogr., Sect. D* **2002**, *58*, 1442.